Hindawi Publishing Corporation
Journal of Nanomaterials
Volume 2015, Article ID 231848, 8 pages
http://dx.doi.org/10.1155/2015/231848

*Research Article*

# Effect of Co Distribution on Plastic Deformation of Nanocrystalline Al-10.2 at.% Co Alloy

**Rita I. Babicheva,[1] Sergey V. Dmitriev,[2,3] Ying Zhang,[4] Shaw Wei Kok,[4] and Kun Zhou[1]**

[1]*School of Mechanical and Aerospace Engineering, Nanyang Technological University, 50 Nanyang Avenue, Singapore 639798*
[2]*Institute for Metals Superplasticity Problems of Russian Academy of Sciences, 39 Khalturin Street, Ufa 450001, Russia*
[3]*Tomsk State University, Lenin Street 36, Tomsk 634036, Russia*
[4]*Singapore Institute of Manufacturing Technology, 71 Nanyang Drive, Singapore 638075*

Correspondence should be addressed to Sergey V. Dmitriev; dmitriev.sergey.v@gmail.com

Received 8 December 2014; Revised 13 January 2015; Accepted 13 January 2015

Academic Editor: Fathallah Karimzadeh



Molecular dynamics is employed to study stress-strain curves obtained during high strain rate deformation of nanocrystalline Al-10.2 at.% Co alloy with (i) randomly distributed Co atoms (Al-Co substitutional solid solution) and (ii) Co atoms segregated in grain boundaries (GBs) of the alloy. The effect of Co distribution, deformation temperature, and the presence of hydrostatic pressure on the stress-strain relation is analyzed. The results are compared to that for nanocrystalline pure Al. It is found that the strength of the Al-Co solid solution is lower than that of the pure Al, while GB segregations of Co increase its strength. The alloys, regardless of the type of Co distribution, under shear loading with no hydrostatic pressure demonstrate higher ductility in comparison with the pure Al. The shear modulus of the Al-Co alloy with the GB segregations is noticeably larger than that of the pure Al and the Al-Co solid solution in a wide range of temperatures. The results of the study show that the GB segregations of Co can have a positive effect on the mechanical properties of nanocrystalline Al.

## 1. Introduction

Metals and alloys subjected to the severe plastic deformation (SPD) have a highly nonequilibrium microstructure with submicron or even nanosize grains. In this form, such materials are often termed as bulk metallic nanomaterials. They demonstrate very high strengths [1–10], enhanced functional properties [1, 2, 11–14], and superplasticity [1, 2, 15, 16] and thus have a great potential in many applications.

The limitations of the metallic bulk nanomaterials are low ductility, thermal stability, and deformability at ambient conditions [1, 2]. Mechanical and functional properties of bulk nanocrystalline Al and other metals can be further improved via alloying with other elements. As a result, not only structures but also physical and mechanical properties such as strength and ductility of bulk nanomaterials can be affected [8, 17–24]. Mechanical and functional characteristics of metallic materials depend on many factors, for instance, the average grain size [1, 2], the nature of interatomic bonding [18], crystallographic orientation [19], porosity [20, 25, 26], presence of lattice defects [27], or amorphous phase [28]. It was observed that the elastic moduli of polycrystalline metals decrease with the reduction of their average grain size [29–32].

The effect of alloying elements on the mechanical properties of a bulk nanomaterial depends on their solubilities, concentrations [33], and distribution within it. During thermomechanical treatment of Al alloys, some of the alloying elements prefer to segregate on grain boundaries (GBs) [34], some are distributed randomly in the form of a solute [35], while others form second-phase precipitates or intermetallic compounds [36]. In a coarse-grained Al alloy, SPD can redistribute its alloying elements and lead to formation of their GB segregations [21–24, 37, 38] or it can result in dissolution of the second-phase precipitates or fragmentation of the intermetallic compounds [39, 40]. In addition, it is believed that SPD through high pressure torsion and subsequent short annealing can result not only in the bulk but

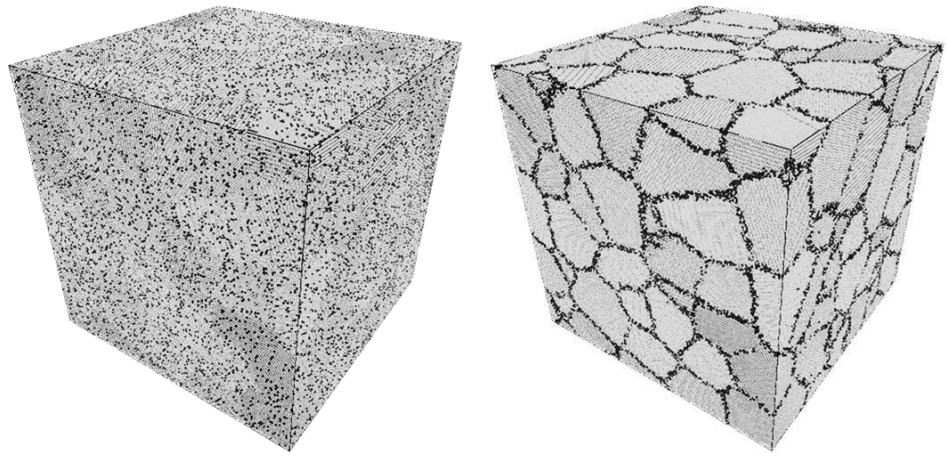

(a) (b)

Figure 1: Nanocrystalline Al-10.2 at.% Co alloys with (a) randomly distributed Co atoms and (b) those segregated in the GBs. Al atoms are represented in light grey, while Co atoms in black.

also in the GB phase transformations, for example, in partial or complete wetting of GB [41–43]. The wetting phase can be either liquid or solid.

Experimentally, it is a great challenge to determine the locations of atoms and compounds of a certain element in the nanocrystalline material [21–24]. However, this challenge can be overcome through atomistic simulations.

The GB segregation energies and the embrittlement potencies for a substitutional Co impurity atom at different atomic positions in the tilt and twist GBs of Al bicrystals were calculated in our recent work [44]. It was shown that the Co impurity atoms tend to remain in these GBs and increase their strength because both the GB segregation energies and the embrittlement potencies are negative for the Co atoms at most of the irreducible positions in the GBs. Having these results in mind it is tempting to study the effect of the GB segregations of Co on the yield stress and thermal stability of the shear modulus of nanocrystalline Al-Co alloy at different deformation temperatures. The present study focuses on the comparison of these results with those obtained for the nanocrystalline pure Al and its alloy with random distribution of the Co atoms.

## 2. Modeling

A three-dimensional cuboidal computational cell with the edge of 42 nm contains about 4.6 million atoms. Using the Voronoi procedure [10, 25, 44–46], the cell volume is divided into 100 randomly oriented face-centered cubic (fcc) Al grains with the average size of about 11 nm. The Al (Co) atom has the radius of 143 (125) pm [47]. Two types of the Al-Co alloys are obtained through the substitution of the Al atoms by the Co atoms. Random substitution of 10.2% of the Al atoms of the computational cell, regardless their coordination numbers, results in the Al-10.2 at.% Co substitutional solid solution (Figure 1(a)). Atoms in the ideal fcc lattice have 12 neighbors but in the vicinity of GBs some atoms have different number of neighbors. Replacement of all the Al atoms having 11 or 10 neighbors by Co atoms results in the Al-10.2 at.% Co alloy with the GB segregations of Co (see Figure 1(b)). Note that the discussion of how such solubility and distributions of the Co atoms can be achieved experimentally is out of the scope of the present study.

The molecular dynamics (MD) simulations are performed using the atomic/molecular massively parallel simulator (LAMMPS) program package [48]. The interatomic forces are modeled with the many-body embedded-atom method potentials [49]. Periodic boundary conditions are applied along the three orthogonal directions of the cuboidal computational cell. The simulations of a shear deformation of the pure Al and its alloys are performed with the NPT ensemble (constant number of atoms, pressure, and temperature).

Initially, the nanocrystalline Al and the Al-Co alloys are relaxed at zero temperature to obtain the state of the minimum potential energy. Then the shear deformation up to shear strain of $\gamma_{xy} = 0.2$ is applied at a constant strain rate of $10^8\,s^{-1}$. The simulations of plastic deformation of the pure Al and its alloys are performed at two different temperatures (300 and 600 K) and the concurrent presence of the hydrostatic pressure of 0 and 6 GPa, while the shear modulus at different temperatures (0, 150, 300, 450, and 600 K) is calculated as the tangent of the stress-strain curves obtained at their shear elastic deformation up to $\gamma_{xy} = 0.005$ and zero hydrostatic pressure.

## 3. Results and Discussion

*3.1. Stress-Strain Curves.* The calculated stress-strain curves $\tau_{xy}(\gamma_{xy})$ for the pure nanocrystalline Al (solid line), the Al-Co solid solution (dotted line), and the Al-Co alloy with the GB segregations of Co (dashed line) are presented in Figure 2. Figures 2(a) and 2(b) show the results for the shear deformation at 300 K, and Figures 2(c) and 2(d) for 600 K. The curves plotted in (a, c) are obtained in the absence of

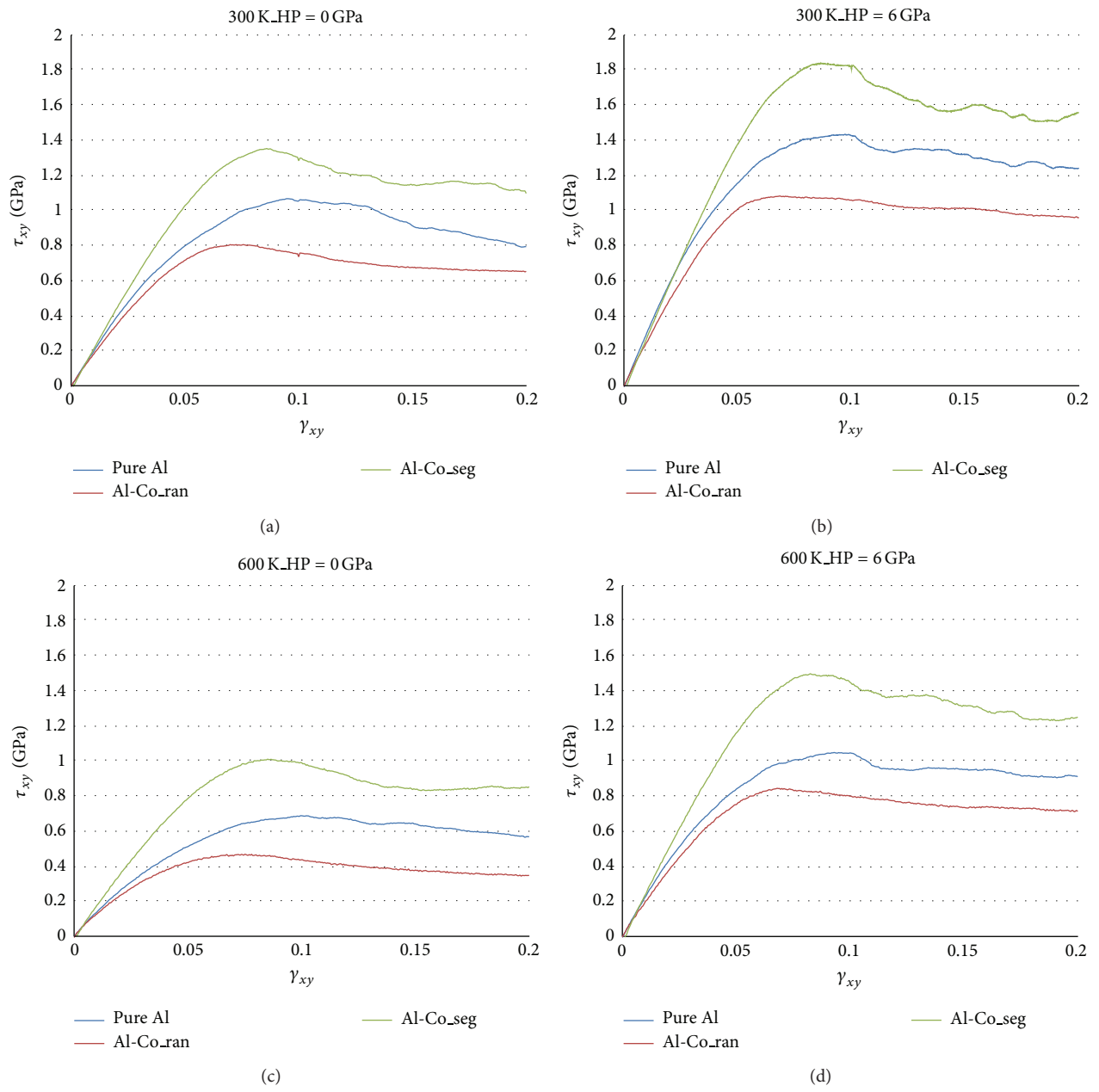


Figure 2: Stress-strain curves for the nanocrystalline pure Al (blue line), Al-Co solid solution (red line), and Al-Co alloy with the GB segregations of Co (green line). For (a, b), the deformation temperature is 300 K, while for (c, d), it is 600 K. The hydrostatic pressure in (a, c) is 0 GPa, while in (b, d), it is 6 GPa.

hydrostatic pressure, while in (b, d) the hydrostatic pressure is equal to 6 GPa.

Notice that at all the considered conditions of plastic deformation, the Al-Co alloy with the GB segregations of Co demonstrates higher strength compared to that of the pure Al, while the strength of the Al-Co solid solution is always lower. Naturally, the increase of temperature results in the reduction of the yield stress, while the increase in the hydrostatic pressure leads to the opposite effect. Among these deformation conditions, the highest yield stress of the pure Al and its alloys can be observed for the temperature of 300 K and the hydrostatic pressure of 6 GPa (Figure 2(b)). Note that such value of the hydrostatic pressure is typically realized during SPD through high-pressure torsion [2]. As expected, the yield stresses are the lowest for the pure Al and the Al-Co alloys after the shear deformation at 600 K and zero hydrostatic pressure (Figure 2(c)). All the curves after reaching a maximum demonstrate slow decrease in stresses with further deformation. This can be explained by the deformation-induced grain growth by means of GB migration and grain rotation, according to the Hall-Petch law [50]. In order to analyze the stress-strain relations of the

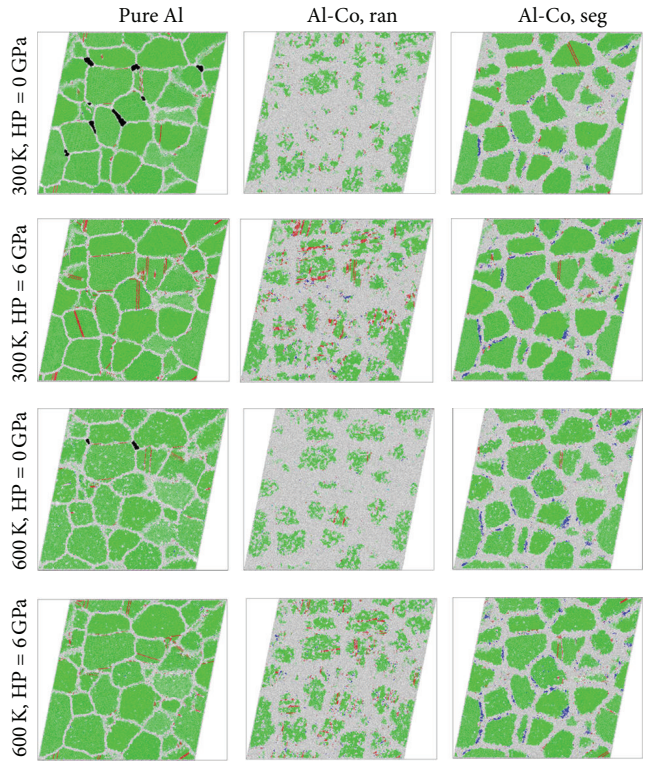


Figure 3: Common neighbor analysis of the structures for the pure Al and its alloys in the $x$-$y$-plane at 20% shear deformation. The regions with the fcc, hexagonal close packed (hcp), body-centered cubic (bcc), and other (undetermined) areas are colored in green, red, blue, and grey, respectively. The left, middle, and right columns show the results for the pure Al, Al-Co solid solution, and Al-Co alloy with the GB segregations, respectively. For each row, the deformation conditions are shown on the left of the structures. Voids are colored in black.

studied materials, their microstructures at shear deformation of $\gamma_{xy} = 0.2$ are studied.

*3.2. Microstructure at 20% Shear Deformation.* The atom common neighbor analysis of the studied materials' structures at 20% shear strain in the $x$-$y$-plane is carried out. The obtained results for the pure Al, Al-Co solid solution, and Al-Co alloy with the GB segregations of Co are shown in the left, middle, and right columns of Figure 3, respectively.

The analysis for the nanocrystalline pure Al (Figure 3, left column) reveals that at the shear strain of 20% the fcc coordination of atoms prevails inside the grains, especially at the deformation temperature of 300 K. At 600 K, due to large thermal fluctuations the crystal structure in some regions inside grains is indefinite. It is noticeable that the width of GBs is larger at the deformation temperature of 600 K as compared to 300 K. The red regions which correspond to the hcp lattice in the structures reveal the appearance of stacking faults and indicate some dislocation activity which is highest at 300 K and the hydrostatic pressure of 6 GPa. The deformation at 600 K, regardless of the presence of the hydrostatic pressure, results in the change of GBs' positions with respect to those for the structure after the low temperature deformation meaning that the pure Al undergoes the GB migraton and has low thermal stability.

The Al-Co solid solution undergoes strong amorphization during the shear plastic deformation (Figure 3, middle column) [51]. Indeed, a large portion of the atoms is colored in grey with the indefinite crystal structure. Interestingly, the presence of hydrostatic pressure somewhat decreases the areas with the amorphous structure.

The Al-Co alloy with the Co atoms located in GBs (Figure 3, right column) undergoes the amorphization only in the regions close to GBs which are rich in Co. The dislocation activity can be noticed inside grains but it is weaker than that in the case of the pure Al. Unlike the pure Al, the Al-Co alloy with the GB segregations does not undergo any GB motion during high temperature deformation implying that the GB segregations increase the thermal stability of the alloy. Structures presented in the right column of Figure 3 confirm the possibility of the GB phase transformations discussed, for example, in a series of works by Straumal et al. [41–43].

Due to the formation of voids (Figure 3, shown in black), the nanocrystalline pure Al has smaller ductility than the Al-Co alloys. It should be noticed that the voids appear only in the pure Al deformed in the absence of the hydrostatic pressure. The void formation is more intensive in the case of lower deformation temperature.

Figure 4 shows $\tau_{xy}$ shear stress distribution at $\gamma_{xy} = 0.2$ in (a) the nanocrystalline pure Al, (b) Al-Co solid solution, and (c) Al-Co alloy with the GB segregations of Co. The deformation conditions are 300 K and no hydrostatic pressure. The voids in Figure 4(a) are highlighted in black. In Figures 4(a) and 4(c), the high shear stresses can be seen

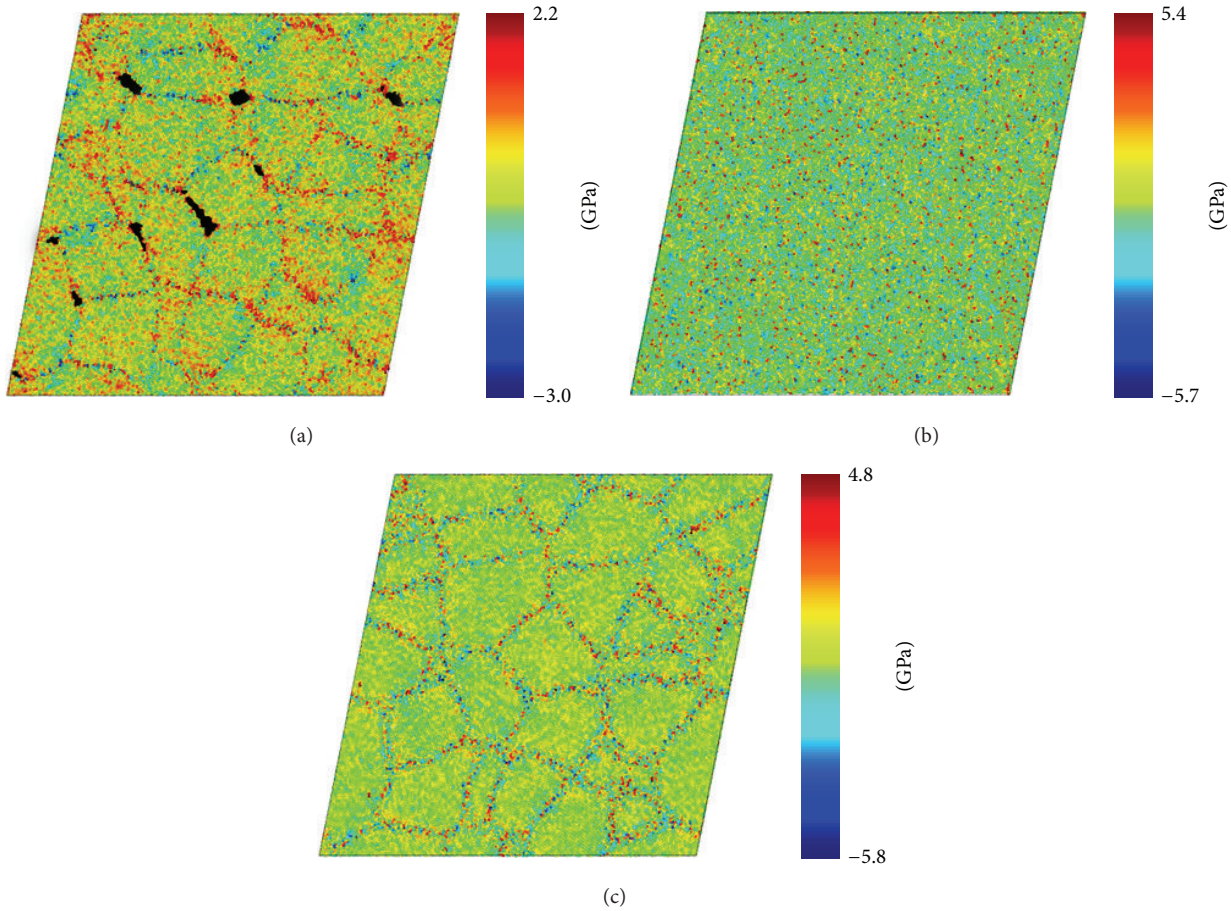


FIGURE 4: Shear stress distribution at $\gamma_{xy} = 0.2$ in (a) the nanocrystalline pure Al, (b) Al-Co solid solution, and (c) Al-Co alloy with the GB segregations of Co. Black regions in (a) show the voids.

mainly along the GBs, while in Figure 4(b) they are scattered all over the presented cross-section area. Figure 4(b) also reflects that such random distribution of high level stresses in the Al-Co solid solution results in its amorphization during shear plastic deformation. Interestingly, that along with the atoms having very high stresses and distributed randomly along GBs of the Al-Co alloy with the GB segregations the regions near the GBs have very low stresses (Figure 4(c)).

*3.3. Shear Modulus.* Figure 5 shows the shear modulus $\mu$ as the function of temperature at zero hydrostatic pressure for the nanocrystalline pure Al (solid line with no symbols), Al-Co solid solution (open dots), and Al-Co alloy with GB segregations of Co (filled dots). At 0 K, both the alloys have $\mu$ higher than that for the pure Al. For the Al-Co solid solution the increase in the rigidity is about 4%, while for the Al-Co alloy with the GB segregations of Co, it is about 16%. For all the three materials, as expected, the shear modulus decreases with temperature. For elevated temperatures, the Al-Co solid solution has the lowest $\mu$, while for the Al-Co alloy with the GB segregations, it remains the highest. At 600 K, the shear modulus of the Al-Co alloy with the GB segregations is 51% larger than that of the pure Al demonstrating the highest thermal stability of $\mu$.

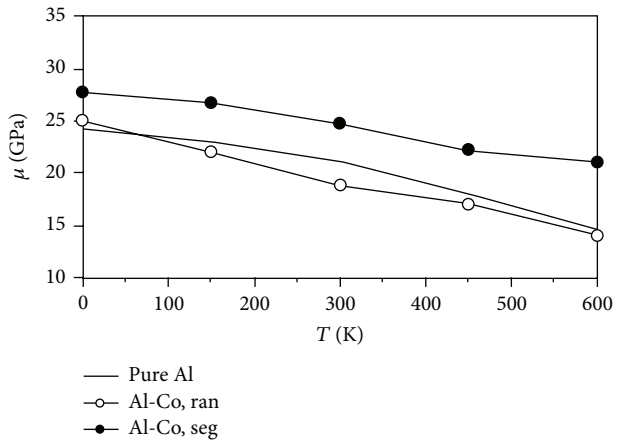


FIGURE 5: Shear modulus $\mu$ as a function of temperature for the nanocrystalline pure Al (solid line with no symbols), Al-Co solid solution (open dots), and Al-Co alloy with the GB segregations of Co (filled dots).

## 4. Conclusions and Future Problems

The paper studies the effect of deformation temperature and the hydrostatic pressure on stress-strain responses of the

nanocrystalline pure Al, Al-10.2 at.% Co solid solution, and Al-10.2 at.% Co alloy with the Co atoms segregated along the GBs during their shear plastic deformation via the MD simulations. Evolution of the microstructure during shear deformation was analyzed and the temperature dependence of the shear modulus was calculated for all the three studied materials.

In contrast to the Al-Co solid solution, the Al-Co alloy with the Co distributed along GBs has an enhanced strength as well as the structure thermal stability in comparison with the pure Al. In particular, the Al-Co alloy with the GB segregation of Co (Al-Co solid solution) at the low temperature shear deformation (300 K) with the concurrent presence of the hydrostatic pressure of 6 GPa demonstrates the maximal shear stress which is 27% higher (28% lower) than that for the nanocrystalline pure Al.

Unlike the Al-Co alloys, regardless of the Co atom distribution, in the nanocrystalline pure Al deformed in the absence of the hydrostatic pressure at shear strain of $\gamma_{xy} = 0.2$ the voids formation can be observed. The void nucleation is more intensive in the case of the low temperature deformation. Thus, the pure Al has smaller ductility than for the considered alloys.

The GB segregations of the Co atoms in the Al-Co alloy increase the shear modulus at 0 K and its thermal stability.

The presence of the Co atoms leads to the amorphization of the Al-Co alloys and can result in the GB phase transformations [41–43] (see Figure 3, right column).

To the best of our knowledge, the effect of GB wetting has not been yet addressed in MD study. It is tempting to apply this powerful method to the analysis of GB transformations in such alloys as Al-Zn [41, 43] or Cu-Co [42].

Notice that in this study, the shear deformation is applied to the nanocrystalline structures that are free of internal stresses. In practice, however, bulk nanocrystalline materials obtained by SPD and disperse metallic nanomaterials containing defects, such as dislocations and disclinations, are characterized by the presence of high residual stresses [52–56]. The study of mechanical characteristics of Al alloys with the residual stresses and comparison of the results with those presented here is another interesting direction for a future work.

## Conflict of Interests

The authors declare that there is no conflict of interests regarding the publication of this paper.

## Acknowledgments

The work is supported by the SIMTech-NTU Joint Lab on Reliability, Singapore. Rita I. Babicheva acknowledges the Singapore International Graduate Award (SINGA) for providing her Ph.D. scholarship. For Sergey V. Dmitriev this research carried out in 2014-2015 was supported by "The Tomsk State University Academic D.I. Mendeleev Fund Program."

## References

[1] R. Z. Valiev, A. P. Zhilyaev, and T. G. Langdon, *Bulk Nanostructured Materials: Fundamentals and Applications*, John Wiley & Sons, Hoboken, NJ, USA, 2014.

[2] A. P. Zhilyaev and T. G. Langdon, "Using high-pressure torsion for metal processing: fundamentals and applications," *Progress in Materials Science*, vol. 53, no. 6, pp. 893–979, 2008.

[3] M. Zehetbauer, R. Grössinger, H. Krenn et al., "Bulk nanostructured functional materials by severe plastic deformation," *Advanced Engineering Materials*, vol. 12, no. 8, pp. 692–700, 2010.

[4] Y. Estrin and A. Vinogradov, "Extreme grain refinement by severe plastic deformation: a wealth of challenging science," *Acta Materialia*, vol. 61, no. 3, pp. 782–817, 2013.

[5] R. Z. Valiev and T. G. Langdon, "The art and science of tailoring materials by nanostructuring for advanced properties using SPD techniques," *Advanced Engineering Materials*, vol. 12, no. 8, pp. 677–691, 2010.

[6] R. Z. Valiev, I. Sabirov, A. P. Zhilyaev, and T. G. Langdon, "Bulk nanostructured metals for innovative applications," *JOM*, vol. 64, no. 10, pp. 1134–1142, 2012.

[7] Z. X. Wu, Y. W. Zhang, M. H. Jhon, J. R. Greer, and D. J. Srolovitz, "Nanostructure and surface effects on yield in Cu nanowires," *Acta Materialia*, vol. 61, no. 6, pp. 1831–1842, 2013.

[8] O. Sitdikov, E. Avtokratova, R. Babicheva, T. Sakai, K. Tsuzaki, and Y. Watanabe, "Influence of processing regimes on fine-grained microstructure development in an AlMgSc alloy by hot equal-channel angular pressing," *Materials Transactions*, vol. 53, no. 1, pp. 56–62, 2012.

[9] O. S. Sitdikov, E. V. Avtokratova, and R. I. Babicheva, "Effect of temperature on the formation of a microstructure upon equal-channel angular pressing of the Al-Mg-Sc 1570 alloy," *The Physics of Metals and Metallography*, vol. 110, no. 2, pp. 153–161, 2010.

[10] D. V. Bachurin and P. Gumbsch, "Elastic and plastic anisotropy after straining of nanocrystalline palladium," *Physical Review B—Condensed Matter and Materials Physics*, vol. 85, no. 8, Article ID 085407, 2012.

[11] R. K. Khisamov, I. M. Safarov, R. R. Mulyukov, and Y. M. Yumaguzin, "Effect of grain boundaries on the electron work function of nanocrystalline nickel," *Physics of the Solid State*, vol. 55, no. 1, pp. 1–4, 2013.

[12] T. Shanmugasundaram, M. Heilmaier, B. S. Murty, and V. S. Sarma, "On the Hall-Petch relationship in a nanostructured Al-Cu alloy," *Materials Science and Engineering A*, vol. 527, no. 29-30, pp. 7821–7825, 2010.

[13] R. K. Khisamov, Y. M. Yumaguzin, R. R. Mulyukov et al., "Effect of a crystalline structure on the ion-electron emission of the Al + 6% Mg alloy," *Technical Physics Letters*, vol. 39, no. 3, pp. 265–267, 2013.

[14] J. Zhang, Y. N. Huang, C. Mao, and P. Peng, "Structural, elastic and electronic properties of $\theta$ ($Al_2Cu$) and S ($Al_2CuMg$) strengthening precipitates in Al-Cu-Mg series alloys: first-principles calculations," *Solid State Communications*, vol. 152, no. 23, pp. 2100–2104, 2012.

[15] E. Avtokratova, O. Sitdikov, M. Markushev, and R. Mulyukov, "Extraordinary high-strain rate superplasticity of severely deformed Al–Mg–Sc–Zr alloy," *Materials Science and Engineering A*, vol. 538, pp. 386–390, 2012.

[16] M. Zha, Y. Li, R. H. Mathiesen, R. Bjørge, and H. J. Roven, "Achieve high ductility and strength in an Al-Mg alloy by severe

plastic deformation combined with inter-pass annealing," *Materials Science and Engineering A*, vol. 598, pp. 141–146, 2014.

[17] U. F. Al-Qawabeha and S. M. Al-Qawabah, "Effect of roller burnishing on pure aluminum alloyed by copper," *Industrial Lubrication and Tribology*, vol. 65, no. 2, pp. 71–77, 2013.

[18] J. Wang, S.-L. Shang, Y. Wang et al., "First-principles calculations of binary Al compounds: enthalpies of formation and elastic properties," *Calphad*, vol. 35, no. 4, pp. 562–573, 2011.

[19] W. Zhou, L. Liu, B. Li, Q. Song, and P. Wu, "Structural, elastic, and electronic properties of Al-Cu intermetallics from first-principles calculations," *Journal of Electronic Materials*, vol. 38, no. 2, pp. 356–364, 2009.

[20] R. Zugic, B. Szpunar, V. D. Krstic, and U. Erb, "Effect of porosity on the elastic response of brittle materials: an embedded-atom method approach," *Philosophical Magazine A*, vol. 75, no. 4, pp. 1041–1055, 1997.

[21] X. Sauvage, A. Ganeev, Y. Ivanisenko, N. Enikeev, M. Murashkin, and R. Valiev, "Grain boundary segregation in UFG alloys processed by severe plastic deformation," *Advanced Engineering Materials*, vol. 14, no. 11, pp. 968–974, 2012.

[22] I. Sabirov, M. Y. Murashkin, and R. Z. Valiev, "Nanostructured aluminium alloys produced by severe plastic deformation: new horizons in development," *Materials Science and Engineering A*, vol. 560, pp. 1–24, 2013.

[23] X. Sauvage, N. Enikeev, R. Valiev, Y. Nasedkina, and M. Murashkin, "Atomic-scale analysis of the segregation and precipitation mechanisms in a severely deformed Al-Mg alloy," *Acta Materialia*, vol. 72, pp. 125–136, 2014.

[24] M. M. Abramova, N. A. Enikeev, R. Z. Valiev et al., "Grain boundary segregation induced strengthening of an ultrafine-grained austenitic stainless steel," *Materials Letters*, vol. 136, pp. 349–352, 2014.

[25] J. Schiøtz, T. Vegge, F. D. Di Tolla, and K. W. Jacobsen, "Atomic-scale simulations of the mechanical deformation of nanocrystalline metals," *Physical Review B—Condensed Matter and Materials Physics*, vol. 60, no. 17, pp. 11971–11983, 1999.

[26] D. V. Bachurin and P. Gumbsch, "Atomistic simulation of the deformation of nanocrystalline palladium: the effect of voids," *Modelling and Simulation in Materials Science and Engineering*, vol. 22, no. 2, Article ID 025011, 2014.

[27] X. Tingdong and Z. Lei, "The elastic modulus in the grain-boundary region of polycrystalline materials," *Philosophical Magazine Letters*, vol. 84, no. 4, pp. 225–233, 2004.

[28] R. I. Babicheva and K. Y. Mulyukov, "Thermomechanical treatment to achieve stable two-way shape memory strain without training in Ti-49.8 at.% Ni alloy," *Applied Physics A*, vol. 116, no. 4, pp. 1857–1865, 2014.

[29] A. Latapie and D. Farkas, "Effect of grain size on the elastic properties of nanocrystalline $\alpha$-iron," *Scripta Materialia*, vol. 48, no. 5, pp. 611–615, 2003.

[30] S.-J. Zhao, K. Albe, and H. Hahn, "Grain size dependence of the bulk modulus of nanocrystalline nickel," *Scripta Materialia*, vol. 55, no. 5, pp. 473–476, 2006.

[31] Y. Zhou, S. van Petegem, D. Segers, U. Erb, K. T. Aust, and G. Palumbo, "On Young's modulus and the interfacial free volume in nanostructured Ni-P," *Materials Science and Engineering A*, vol. 512, no. 1-2, pp. 39–44, 2009.

[32] M. Grewer, J. Markmann, R. Karos, W. Arnold, and R. Birringer, "Shear softening of grain boundaries in nanocrystalline Pd," *Acta Materialia*, vol. 59, no. 4, pp. 1523–1529, 2011.

[33] M. Abo-Elsoud, H. Esmail, and M. S. Sobhy, "Correlation between elastic modulus of Al-Cu alloys and metallurgical characteristics of their constituent elements," *Radiation Effects and Defects in Solids*, vol. 162, no. 9, pp. 685–690, 2007.

[34] G. Sha, S. P. Ringer, Z. C. Duan, and T. G. Langdon, "An atom probe characterisation of grain boundaries in an aluminium alloy processed by equal-channel angular pressing," *International Journal of Materials Research*, vol. 100, no. 12, pp. 1674–1678, 2009.

[35] R. Fernández and G. González-Doncel, "A unified description of solid solution creep strengthening in Al-Mg alloys," *Materials Science and Engineering A*, vol. 550, pp. 320–324, 2012.

[36] A. Villuendas, J. Jorba, and A. Roca, "The role of precipitates in the behavior of Young's modulus in aluminum alloys," *Metallurgical and Materials Transactions A*, vol. 45, no. 9, pp. 3857–3865, 2014.

[37] P. V. Liddicoat, X. Z. Liao, Y. H. Zhao et al., "Nanostructural hierarchy increases the strength of aluminium alloys," *Nature Communications*, vol. 1, article 63, 2010.

[38] R. Ferragut, P. V. Liddicoat, X.-Z. Liao et al., "Chemistry of grain boundary environments in nanocrystalline Al 7075," *Journal of Alloys and Compounds*, vol. 495, no. 2, pp. 391–393, 2010.

[39] I. G. Brodova, I. G. Shirinkina, A. N. Petrova, O. V. Antonova, and V. P. Pilyugin, "Evolution of the structure of V95 aluminum alloy upon high-pressure torsion," *The Physics of Metals and Metallography*, vol. 111, no. 6, pp. 630–638, 2011.

[40] J. Crump, X. G. Qiao, and M. J. Starink, "The effect of high-pressure torsion on the behaviour of intermetallic particles present in Al-1Mg and Al-3Mg," *Journal of Materials Science*, vol. 47, no. 4, pp. 1751–1757, 2012.

[41] B. Straumal, R. Valiev, O. Kogtenkova et al., "Thermal evolution and grain boundary phase transformations in severely deformed nanograined Al-Zn alloys," *Acta Materialia*, vol. 56, no. 20, pp. 6123–6131, 2008.

[42] B. B. Straumal, A. Korneva, O. Kogtenkova et al., "Grain boundary wetting and premelting in the Cu-Co alloys," *Journal of Alloys and Compounds*, vol. 615, supplement 1, pp. S183–S187, 2014.

[43] B. B. Straumal, X. Sauvage, B. Baretzky, A. A. Mazilkin, and R. Z. Valiev, "Grain boundary films in Al-Zn alloys after high pressure torsion," *Scripta Materialia*, vol. 70, no. 1, pp. 59–62, 2014.

[44] R. I. Babicheva, S. V. Dmitriev, Y. Zhang et al., "Effect of grain boundary segregations of Fe, Co, Cu, Ti, Mg and Pb on small plastic deformation of nanocrystalline Al," *Computational Materials Science*, vol. 98, pp. 410–416, 2015.

[45] S. Brandstetter, P. M. Derlet, S. Van Petegem, and H. van Swygenhoven, "Williamson-Hall anisotropy in nanocrystalline metals: X-ray diffraction experiments and atomistic simulations," *Acta Materialia*, vol. 56, no. 2, pp. 165–176, 2008.

[46] D. V. Bachurin and P. Gumbsch, "Atomistic simulation of straining of nanocrystalline palladium," *Acta Materialia*, vol. 58, pp. 5491–5501, 2010.

[47] R. J. Gillespie, D. A. Humphreys, N. C. Baird, and E. A. Robinson, *Chemistry*, Allyn & Bacon, Newton, Mass, USA, 1986.

[48] S. Plimpton, "Fast parallel algorithms for short-range molecular dynamics," *Journal of Computational Physics*, vol. 117, no. 1, pp. 1–19, 1995.

[49] M. S. Daw and M. I. Baskes, "Embedded-atom method: derivation and application to impurities, surfaces, and other defects in metals," *Physical Review B*, vol. 29, no. 12, pp. 6443–6453, 1984.

[50] E. A. Korznikova and S. V. Dmitriev, "Mechanisms of deformation-induced grain growth of a two-dimensional nanocrystal at different deformation temperatures," *The Physics of Metals and Metallography*, vol. 115, no. 6, pp. 570–575, 2014.

[51] S. Ogut and K. M. Rabe, "Ab initio pseudopotential calculations for aluminum-rich cobalt compounds," *Physical Review B*, vol. 50, no. 4, pp. 2075–2084, 1994.

[52] K. Zhou, A. A. Nazarov, and M. S. Wu, "Competing relaxation mechanisms in a disclinated nanowire: temperature and size effects," *Physical Review Letters*, vol. 98, no. 3, Article ID 035501, 2007.

[53] M. S. Wu, A. A. Nazarov, and K. Zhou, "Misorientation dependence of the energy of [1–100] symmetrical tilt boundaries in hcp metals: prediction by the disclination-structural unit model," *Philosophical Magazine*, vol. 8, pp. 785–806, 2004.

[54] M. S. Wu, K. Zhou, and A. A. Nazarov, "Crack nucleation at disclinated triple junctions," *Physical Review B: Condensed Matter and Materials Physics*, vol. 76, no. 13, Article ID 134105, 2007.

[55] K. Zhou, A. A. Nazarov, and M. S. Wu, "Continuum and atomistic studies of a disclinated crack in a bicrystalline nanowire," *Physical Review B—Condensed Matter and Materials Physics*, vol. 73, no. 4, Article ID 045410, 2006.

[56] R. I. Babicheva, K. A. Bukreeva, S. V. Dmitriev, R. R. Mulyukov, and K. Zhou, "Strengthening of NiAl nanofilms by introducing internal stresses," *Intermetallics*, vol. 43, pp. 171–176, 2013.